Structure, thermochemistry, and conformational analysis of peroxides ROOR and hydroperoxides ROOH (R = Me, Bu^t, CF_3)

S. L. Khursan[a] and V. L. Antonovsky[b]★

[a]*Bashkir State University,*
32 ul. Frunze, 450074 Ufa, Russian Federation.
Fax: +7 (347 2) 22 6105
[b]*N. N. Semenov Institute of Chemical Physics, Russian Academy of Sciences,*
4 ul. Kosygina, 119991 Moscow, Russian Federation.
Fax: +7 (095) 938 2156. E-mail: kasaikina@chph.ras.ru

The equilibrium structures, total energies, and harmonic frequencies of peroxides ROOR and ROOH (R = Me, Bu^t, CF_3) were calculated using the perturbation theory (MP4//MP2 method) and density functional approach (B3LYP) in the 6-31G(d,p) basis set. The conformational flexibility of peroxides under rotation about the O-O bond was investigated. It was found that the stable conformation of a peroxide molecule is determined by superposition of the destabilizing effects (repulsion between the lone electron pairs, steric hindrances) and the interaction of the nonbonding orbitals of oxygen atoms with the antibonding orbitals of the adjacent polar bonds. The latter effect stabilizes the nonplanar structure of the peroxide molecule. The role of orbital interactions in manifestation of the d-effect (distortion of the tetrahedral configuration of the X_3CO fragment of peroxide molecule) was revealed. The vibrational spectra of peroxides were calculated and compared with the experimental data. The potential energy distribution over normal vibrations was analyzed. The enthalpies of formation and the bond strengths in the molecules of compounds examined were calculated in the framework of the isodesmic reaction approach.

Key words: organic peroxides, nonempirical quantum-chemical calculations, structure, conformational analysis, vibrational spectra, enthalpies of formation.

Compounds containing the O—O group and originating from dioxygen, the major active component of the Earth atmosphere, play an important role in many natural processes. Involvement of these compounds in the combustion, oxidation, radical polymerization, and other reactions that use their oxidizing property, as well as the ability to undergo a ready decomposition into free radicals, have predetermined a broad spectrum of scientific and industrial applications of organic peroxides. The variety of structures and high reactivity have permitted the use of peroxides as model objects for investigations of many fundamental problems of chemistry.[1—7] Relatively high lability of peroxide compounds, which readily decompose *via* homolysis of the peroxide bond, precludes investigations of their structure, physicochemical properties as well as the spectral and thermodynamic characteristics (in particular, enthalpies of formation and bond dissociation energies). Experimental data on the structure of organic peroxides were collected in a review[8] from which it follows that the structure and conformational behavior of peroxides have been studied rather poorly. Besides, investigations of the structure of peroxide molecules by gas-phase electron diffraction and X-ray diffraction analysis revealed some peculiar features that are common to all peroxides and require theoretical substantiation. The vibrational spectra of organic peroxides also have not been adequately studied. Different authors have reported different band assignments to particular types of vibrations (see, *e.g.*, Ref. 9). The enthalpies of formation of organic peroxides have been determined mainly in the condensed phase.[10] Information on the peroxides with relatively simple structures (alkyl peroxides, alkyl hydroperoxides, peroxy acids, peroxy esters, *etc.*), which are the first members of the corresponding homologous series, is rather scarce. In this connection quantum-chemical calculations based on modern theoretical concepts can be used as supplementary to the experimental investigations on the chemical nature of peroxides. Such calculations provide an efficient tool for the determination of many physicochemical characteristics with the accuracy comparable to that achieved in the experiments. Earlier, we have studied the conformational flexibility of a num-

Published in Russian in *Izvestiya Akademii Nauk. Seriya Khimicheskaya,* No. 6, pp. 1241—1253, June, 2003.

1066-5285/03/5206-1312 $25.00

ber of peroxy nitrates[11—14] and calculated the O—O and O—H bond strengths in various peroxides[15] as well as in trioxides and hydrotrioxides.[16,17] We plan to perform quantum-chemical studies of the properties of the most important classes of peroxides. In this work (for preliminary communication, see Ref. 18) we report on the study of physicochemical parameters of alkyl peroxides and hydroperoxides. To reveal the characteristic features of the molecular structure and the effect of substituents on the properties of peroxides, compounds ROOH (**1—3**) and ROOR (**4—6**) containing the electron-donor (R = Me (**1**, **4**), Bu^t (**2**, **5**)) and electron-acceptor (R = CF_3 (**3**, **6**)) substituents were studied.

Calculation Procedure

Procedure for quantum-chemical calculations. The *ab initio* and density functional (DFT) quantum-chemical calculations were carried out using the GAMESS [19] and GAUSSIAN-98 [20] programs. Molecules and radicals were calculated by the restricted (RHF) and unrestricted (UHF) Hartree—Fock method, respectively. Density functional calculations were performed using the B3LYP hybrid functional.[21] The RHF calculations were carried out with inclusion of electron correlation at the second (MP2) and fourth order (MP4) Møller—Plesset level of perturbation theory. All calculations were performed with the 6-31G(d,p) basis set (6-31G split-valence basis set augmented with polarization d-functions for the non-hydrogen atoms and p-functions for H atoms).

The ground-state geometries of molecules **1** and **4** were determined by the RHF/6-31G(d,p), MP2/6-31G(d,p), and B3LYP/6-31G(d,p) methods with full optimization of all geometric parameters. In other cases, the MP2/6-31G(d,p) and B3LYP/6-31G(d,p) approximations were employed. The potential curves of internal rotation about the peroxide bond for the compounds under study were obtained from calculations with the constant value of the dihedral, or torsion, angle φ, which characterizes the mutual arrangement of the atoms in the C—O—O—H (or C—O—O—C) fragment (Fig. 1), and full optimization of the remaining geometric parameters. These calculations were carried out with a φ increment of 10 or 15° in the range 0—180° with allowance for symmetry considerations. The

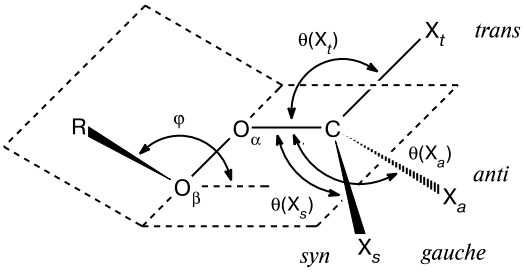

Fig. 1. Schematic representation of the peroxide molecule and the most important angles in its structure: φ is the torsion angle between the COO and OOR planes, $\theta(X_t)$ is the transoid bond angle, and $\theta(X_s)$ and $\theta(X_a)$ are the *gauche*-angles for the *syn*- and *anti*-oriented atoms (with respect to the substituent R).

geometry of the dialkyl peroxide molecules was optimized assuming C_2 symmetry, which permitted, especially in the case of molecule **5**, a substantial reduction of the computational cost.

The relative energy of a particular conformer was calculated as the energy difference between the given state and the ground state of the molecule. In performing MP2 optimization, the relative energies of different molecular states were also estimated at the MP4-SDQ level of perturbation theory by carrying out single-point calculations for fixed geometry with the 6-31G(d,p) basis set in the "frozen core" approximation.

Calculations of the ground states of the peroxide molecules and peroxy radicals included the solution to the vibrational problem and determination of the force constants, vibrational frequencies (ν), and zero-point vibrational energy corrections (ZPE). When comparing the results of calculations with the published data, the calculated ν and ZPE values were corrected by multiplying them by the corresponding scale factor.[22]

To interpret structural peculiarities of the compounds under study using the bonding orbital populations and the molecule-stabilizing orbital effects, the natural bonding orbital (NBO) approach[23] was employed in the framework of the B3LYP/6-31G(d,p) approximation.

Choice of computational method. The quantum-chemical methods were chosen using the following assessment criteria:

— correct calculations of geometric parameters;

— correct and reliable calculations of the energy of the molecules;

— good cost/efficiency ratio.

The results of the RHF/6-31G(d,p) and DFT/6-31G(d,p) calculations of the equilibrium structures of the methyl peroxide and dimethyl peroxide molecules are listed in Table 1. Comparison with the experiment shows that the RHF method underestimates the O—O and C—O interatomic distances by 0.05—0.06 and 0.02—0.04 Å, respectively. The O—H distance in molecule **1** is also underestimated by 0.02 Å. In contrast to this, the C—O—O and O—O—H bond angles are somewhat overestimated. The inclusion of electron correlation allows one to achieve much better agreement between the theory and experiment, thus providing a way for correct reproduction of all geometric parameters, except for the O—O bond length overestimated by 0.015—0.028 Å (according to MP2 calculations). Augmentation of the basis set with polarization p-functions improves agreement between the results of calculations and experimental data, though the corresponding effect is insignificant.

Among the most important geometric characteristic peroxide molecules is the torsion angle φ between the planes passing through the C, O, O atoms and the O, O, C/H atoms (see Fig. 1). For molecule **1** all the computational methods employed predict the *gauche*-conformation with the φ angle lying in the range 115.2—122.1°, which is in reasonable agreement with the experimental value (114°). In the case of molecule **4** the situation becomes more complicated. Experiments showed[27] that the dimethyl peroxide molecule mainly adopts the *anti*-clinal conformation (φ = 119°). However, the RHF calculations predict the *trans*-arrangement of the Me groups relative to the O—O bond. The inclusion of electron correlation by the MP2 method leads to a strongly flattened $E_{tot}(\varphi)$ dependence with two minima. According to calculations with the 6-31G(d) basis set, the deeper energy minimum corresponds to the structure with φ = 180°, while φ = 124.3° corresponds to the local energy minimum. The inclusion of electron correlation at the

Table 1. Geometric parameters and energy characteristics of the stable conformations of peroxide molecules

Computational method	$-E_{tot}$ /hartree	ZPE	ΔE_{trans}	ΔE_{cis}	Bond length/Å			Angle/deg		
		kJ mol^{-1}			O—O	C—O	O—H	C—O—O	O—O—H	C—O—O—X
					MeOOH (**1**)					
RHF/6-31G(d,p)	189.807567	156.4	1.48	31.5	1.3939	1.3993	0.9460	107.3	102.3	118.6
MP4//MP2/6-31G(d,p)	190.350155	147.5	1.35	30.1	1.4695	1.4203	0.9696	104.5	98.4	122.1
B3LYP/6-31G(d,p)	190.856305	143.8	1.58	27.3	1.4565	1.4168	0.9713	106.1	99.8	115.2
Experiment (gas)[24]	—	—	1.05	—	1.443	1.437	0.967	105.7	99.6	114
					Bu^{t}OOH (**2**)					
MP4//MP2/6-31G(d,p)	307.948581	376.1	3.80	33.4	1.4730	1.4464	0.9699	107.7	98.1	115.3
B3LYP/6-31G(d,p)	308.819981	365.3	4.24	30.1	1.4576	1.4503	0.9705	109.2	99.9	110.9
Experiment (crystal)[25]	—	—	—	—	1.472	1.463	1.01	109.6	100	100
					CF_3OOH (**3**)					
MP4//MP2/6-31G(d,p)	487.416576	86.6	7.91	30.3	1.4580	1.3791	0.9718	105.6	99.2	101.3
B3LYP/6-31G(d,p)	488.582798	84.9	7.61	26.5	1.4480	1.3778	0.9739	107.1	100.3	98.6
Experiment (gas)[26]	—	—	—	—	1.447	1.376	0.974	107.6	~100	~95
					MeOOMe (**4**)					
RHF/6-31G(d,p)	228.838203	235.4	—	—	1.3987	1.3968	—	106.0	—	180.0
MP4//MP2/6-31G(d,p)	229.536419	224.3	0.35	52.0	1.4723	1.4210	—	104.3	—	120.1
MP2/6-311+G(d,p)	229.618849	220.9	—	—	1.4591	1.4155	—	104.4		148.1
B3LYP/6-31G(d,p)	230.169083	218.3	0.10	47.0	1.4633	1.4150	—	105.4	—	131.2
Experiment (gas)[27]	—	—	1.05	—	1.457	1.420	—	105.2	—	119
					Bu^{t}OOBu^t (**5**)					
MP4//MP2/6-31G(d,p)	464.733247	678.2	1.03	138	1.4881	1.4441	—	106.1	—	152.0
B3LYP/6-31G(d,p)	466.093920	660.0	0.10	124	1.4728	1.4431	—	107.5	—	161.2
Experiment (crystal)[28]	—	—	—	—	1.478	1.439	—	106.7	—	164
					CF_3OOCF_3 (**6**)					
MP4//MP2/6-31G(d,p)	823.662216	100.79	8.97	72.5	1.4625	1.3931	—	105.0	—	122.0
B3LYP/6-31G(d,p)	825.615302	98.8	8.05	62.6	1.4511	1.3924	—	106.7	—	120.2
Experiment (gas)[29]	—	—	—	—	1.419	1.399	—	107.2	—	123.3

MP4-SDQ level of theory makes the "correct" minimum more distinct. In the MP2/6-31G(d,p) approximation the minimum E_{tot} value was obtained at $\varphi = 120.1°$, though the transoid arrangement of the Me groups also corresponds to a minimum in the conformational curve, which virtually disappears when calculating the energy of molecule **4** by the MP4//MP2/6-31G(d,p) method. Finally, the B3LYP calculations correctly reproduce all geometric parameters except for the C—O—O—C angle, which appears to be unexpectedly strongly overestimated (~131°). Nevertheless, *trans*-dimethyl peroxide corresponds to the top of the barrier to interconversion between the reflection symmetric stable conformations of molecule **4**. Further extension of the basis set provides no significant improvement of the results obtained. In particular, the MP2/6-311+G(d,p) method excellently reproduces the bond lengths and bond angles, but predicts a φ value of 148.1°.

Correctness and reliability of calculations of the energy characteristics were assessed taking the height of the *trans*-barrier as an example. This parameter was calculated as the difference between the total energy of the *trans*-conformation of the peroxide molecule and the energy of the most stable molecular state. For molecule **1** the results of calculations by all the methods employed agree well with the experimental value. In the case of molecule **4** the calculated ΔE_{trans} value is strongly underestimated (see Table 1). It should be noted that the inclusion of zero-point vibrational energy correction for both the ground and transition states of the interconversion has virtually no effect on the ΔE_{trans} value.

Another evaluation procedure involved calculations of the standard enthalpies of formation of compounds **1** and **4** using the isodesmic reaction (IDR) approach.[30] The results of calculations are listed in Table 2. As can be seen, the RHF method reproduces the experimental data poorer than the MP2 and B3LYP methods which seem to provide more reliable and close results. It should be noted that an important condition for correct calculations of the enthalpies of formation is the correct choice of the IDR. The best results, which nearly coincide with the experimental data, were obtained for the IDR

Table 2. Thermal effects of isodesmic reactions ($\Delta H°$/kJ mol^{-1}) and the standard enthalpies of formation ($\Delta H_f°$/kJ mol^{-1}) of the starting peroxides **1—6**

Isodesmic reaction	$\Delta H°$ ($-\Delta H_f°$)			
	HF	MP4//MP2 6-31G(d,p)	B3LYP	Experiment
$MeOOH + H_2O \rightarrow HOOH + MeOH$	24.1	28.9	27.6	—
1	(120.1)	(124.9)	(123.6)	(131.0)[31]
$MeOOH + HOO^{\bullet} \rightarrow HOOH + MeOO^{\bullet}$	1.5	−1.9	−4.0	—
1	(133.4)	(130.0)	(127.9)	(131.0)[31]
$MeOOMe + 2\ H_2O \rightarrow HOOH + 2\ MeOH$	48.4	60.4	54.3	—
4	(104.3)	(116.3)	(110.2)	(125.5)[32]
$MeOOMe + HOOH \rightarrow 2\ MeOOH$	0.2	2.5	−0.9	—
4 **1**	(126.1	(128.4)	(125.0)	(125.5)[32]
$Bu^tOOH + HOO^{\bullet} \rightarrow HOOH + Bu^tOO^{\bullet}$	—	−7.2	−11.3	—
2	—	(248.9)	(244.8)	(244.1)[33,34]
$Bu^tOOH + MeOO^{\bullet} \rightarrow MeOOH + Bu^tOO^{\bullet}$	—	−5.2	−7.3	—
2 **1**	—	(244.4)	(242.4)	(244.1)[33,34]
$Bu^tOOBu^t + HOOH \rightarrow 2\ Bu^tOOH$	—	−5.6	−6.2	—
5 **2**	—	(361.5)	(349.7)	(344.6)[32,34]
$CF_3OOH + HOO^{\bullet} \rightarrow HOOH + CF_3OO^{\bullet}$	—	24.9	26.1	—
3				
$CF_3OOH + MeOO^{\bullet} \rightarrow MeOOH + CF_3OO^{\bullet}$	—	26.7	30.1	—
3 **1**				
$CF_3OOCF_3 + HOOH \rightarrow 2\ CF_3OOH$	—	−14.3	−17.0	—
6 **3**				

with balance of Benson´s groups (see Table 2, the reactions with $HOO^{\bullet}$ and HOOH for the peroxides **1** and **4**, respectively).

Calculations with the 6-31G(d,p) basis set and inclusion of electron correlation in the framework of the perturbation theory as well as the DFT calculations correctly reproduce the vibrational spectra of peroxides **1** and **4**. Almost all vibrations are well localized and the results of calculations are in good agreement with the experiment data.[35,36] For instance, the vibrational frequency of the O—O bond in molecule **1** is 821 cm^{-1} (*cf.* a value of 815 cm^{-1} found from MP2/6-31G(d,p) calculations) and that of the C—O bond is 1026 cm^{-1} (*cf.* a calculated value of 1009 cm^{-1}). Molecule **4** belongs to the C_2 point symmetry group; therefore, the IR spectrum exhibits mainly more intense bands of the asymmetrical vibrations. The peroxide bond vibration at 779 cm^{-1} (772 cm^{-1} according to calculations) is of low intensity in the IR spectrum. In contrast to the assignment[37] based on the experimental data,[36] our quantum-chemical calculations predict that the frequency of the most intense asymmetrical vibration of the C—O bond (999 cm^{-1}) is less than that of the symmetrical vibration of this bond (1016 cm^{-1}). This is probably due to a strong mixing of the ν^s(C—O) vibration with the ν(O—O) vibration, which makes a 16% contribution to the potential energy distribution (PED). Positions of the remaining absorption bands active in the IR spectrum are well reproduced by calculations.

Thus, comparison of the results of calculations of molecules **1** and **4** with the experimental data suggests that the MP4//MP2/6-31G(d,p) and B3LYP/6-31G(d,p) methods meet the criteria listed above. These approximations give close results, which can be treated as an indirect evidence for reliability of the calculated data, and were employed for the study of the remaining peroxide compounds.

Results and Discussion

Structure of molecules 1—6. The calculated values of the main geometric parameters of the peroxide molecules under study are listed in Table 1. They are in reasonable agreement with the experimental data obtained by gas-phase electron diffraction[24,26,27,29] and X-ray diffraction analysis.[25,28] According to calculations, the length of the peroxide bond is virtually independent of the structure of a particular peroxide molecule and lies between 1.45 and 1.49 Å. The largest difference between the results of calculations and experimental data was found for molecule **6** for which d_{exp}(O—O) = 1.419±0.020 Å.[29] The calculated C—O and O—H bond lengths coincide with the corresponding experimental values within the limits of experimental error.

The B3LYP method excellently reproduces the C—O—O and O—O—H bond angles (the calculated values differs from the experimental ones by at most 1°). The MP2 approximation provides a somewhat lower accuracy, though in this case the maximum discrepancy between the predicted values and experimental data is only 2.2°.

The error of determination of the torsion angle φ is also small. The largest deviation from the experimental

value (10—15°) was obtained for molecule **2**. The most reasonable explanation for this discrepancy is that the experimental geometric parameters of the Bu^tOOH molecule (**2**) were determined in the solid phase. It seems likely that intermolecular interactions in the crystal lattice of this hydroperoxide cause the φ angle to decrease. Indeed, the H—O—O—H dihedral angle in the hydrogen peroxide molecule (112±1° in the gas phase[38]) decreases down to 90.2° in the crystal.[8]

The torsion angle is strongly dependent on the nature of the substituent at the C_α atom. Apparently, steric repulsion between bulky Bu^t groups dominates in molecule **5**, being responsible for the increase in the φ angle up to ~160°. At the same time the torsion angle in molecule **3** decreases down to ~100° due to electron-acceptor properties of the F atoms. These examples demonstrate that nonvalent interactions contribute largely to the equilibrium structure of the peroxide molecule. High accuracy of quantum-chemical calculations allows them to be used as an independent method for determination of the structure of organic peroxides and for elucidation of the nature and strength of nonvalent electron interactions (see below).

Thermochemistry of peroxides. Quantum-chemical calculations of the thermal effects of the IDR with balance of Benson´s groups permit reliable theoretical estimation of the thermodynamic characteristics (enthalpy of formation, bond strength) of peroxide compounds.[15] Table 2 lists the thermal effects of some IDR constructed in this manner for the peroxides under study. If no nonvalent interactions occur in the molecules participating in such IDR or if these interactions are mutually cancelled out, the thermal effect the IDR thus constructed must be equal to zero, which holds for **1** and **4** (see Table 2). The nonzero thermal effect, ΔH°, points to stabilization ($\Delta H^\circ > 0$) or destabilization ($\Delta H^\circ < 0$) of reagents as compared to the IDR products.

The ΔH_f° value for **5** was determined using the calculated enthalpy of formation of **2** (−245.1±3.0 kJ mol^{-1}), which is in excellent agreement with the experimental data (see Table 2). The results of our calculations of the enthalpy of formation for di-*tert*-butyl peroxide (**5**) are appreciably different, namely, −361.5 (MP4//MP2) and −349.7 (B3LYP) kJ mol^{-1}. The latter value looks more realistic. First, the IDR for **5** must be exothermic taking into account steric repulsion between the bulky Bu^t radicals. B3LYP-Calculations confirmed this assumption; however, the estimate of ΔH° obtained by the MP4//MP2/6-31G(d,p) method is 5.6 kJ mol^{-1}. Second, using the known value $\Delta H_f^\circ(Bu^tO^\bullet) = -95.4$ kJ mol^{-1} [39] and the results of B3LYP/6-31G(d,p) calculations of the enthalpy of formation for compound **5**, we found that the strength of the peroxide bond, D(O—O), in molecule **5** is 158.9 kJ mol^{-1}. This coincides with the recommended[40] D(O—O) value chosen based on analysis of the studies on the kinetics of gas-phase thermolysis of **5**. Therefore, $\Delta H_f^\circ(\mathbf{5}) = -349.7$ kJ mol^{-1}.

Thermochemistry of the fluorine-containing peroxides and corresponding radicals has been the subject of recent research.[41—44] Nevertheless, the data reported by different authors are often contradictory or exhibit a wide scatter of numerical values. For instance, the enthalpy of formation of compound **3** was reported to lie between −1427 and −1507 kJ mol^{-1}.[44,45] Since the absolute values of the enthalpy of formation of the F,O-containing compounds seem to be unreliable, thermochemical analysis was carried out using the relative values, namely, the thermal effects of the reactions and the bond strengths. For instance, from the data listed in Table 2 it follows that

$$\Delta H_f^\circ(CF_3OO^\bullet) - \Delta H_f^\circ(\mathbf{3}) = 177.1\pm2.6 \text{ kJ mol}^{-1}, \quad (1)$$

$$2\Delta H_f^\circ(\mathbf{3}) - \Delta H_f^\circ(\mathbf{6}) = -154.0\pm3.4 \text{ kJ mol}^{-1}. \quad (2)$$

The O—O bond strength in the molecule of trifluoromethyl peroxide (**3**) is 195.8 kJ mol^{-1} [40] (*cf.* a close value of 198.7 kJ mol^{-1} obtained in a recent experimental study[44]). Using the average value, one gets

$$2\Delta H_f^\circ(CF_3O^\bullet) - \Delta H_f^\circ(\mathbf{6}) = 197.3\pm1.6 \text{ kJ mol}^{-1}. \quad (3)$$

Gas-phase decomposition of compound **6** proceeds by the following reaction equation

$$\underset{\mathbf{6}}{CF_3OOCF_3} \rightleftharpoons CF_3OF + CF_2O.$$

The thermal effect of this reaction was measured earlier.[46] From this it follows

$$\Delta H_f^\circ(CF_3OF) + \Delta H_f^\circ(CF_2O) - \Delta H_f^\circ(\mathbf{6}) = 102.5\pm5.0 \text{ kJ mol}^{-1}. \quad (4)$$

The bond strength, $D(CF_3O—F)$, was calculated using the experimental rate constant for gas-phase thermolysis of CF_3OF [46] corrected for the normal pre-exponent value. The recommended value, $D(CF_3O—F)$ = 200.8±4.2 kJ mol^{-1}, is consistent with the results of various versions of DFT calculations.[44] Therefore, we get

$$\Delta H_f^\circ(CF_3O^\bullet) - \Delta H_f^\circ(CF_3OF) = 121.3\pm4.2 \text{ kJ mol}^{-1}. \quad (5)$$

Finally, from the IDR constructed[44] for CF_3OH we determined the O—H bond strength in the trifluoromethanol molecule (497.1±4.2 kJ mol^{-1}), which is in agreement with an independent theoretical estimate.[47] This allows one to derive yet another relation:

$$\Delta H_f^\circ(CF_3O^\bullet) - \Delta H_f^\circ(CF_3OH) = 279.1\pm4.2 \text{ kJ mol}^{-1}. \quad (6)$$

Equations (1)—(6) contain seven unknowns; therefore, we solved them using the $\Delta H_f^\circ(CF_2O)$ value as a reference. A survey of the published data revealed a wide scatter of the $\Delta H_f^\circ(CF_2O)$ values, namely, −600.8,[48]

−623.8,[49] and −638.9 kJ mol^{-1}.[45] High-level quantum-chemical calculations in the framework of the G2 [50] and G2MP2 [51] computational schemes (in the latter case with the data taken from Ref. 52) gave for $\Delta H_f^\circ(CF_2O)$ the values of −620.0 and −625.4 kJ mol^{-1}, respectively, which supports the result obtained in Ref. 49. The thermal effects, ΔH_f° (in kJ mol^{-1}), determined in this work are listed below (error in calculations was ±7.3 kJ mol^{-1}; the value for CF_2O is a reference).

Compound	CF_2O	$CF_3O^\bullet$	$CF_3OO^\bullet$	CF_3OH	CF_3OF	**3**	**6**
$-\Delta H_f^\circ$	623.8±6.0	650.3	648.9	929.4	771.6	826.0	1497.9

Taking into account the above-mentioned wide scatter of the ΔH_f° values, it is an easy matter to find some data which will "coincide" with the results obtained in this work. However, comparison of the relative values seems to be more correct. For instance, from our results it follows that the O—H bond strength in molecule **3** is 395.1 kJ mol^{-1}. Indeed, it is known[15,53,54] that introduction of an electron-acceptor substituent into the hydroperoxide molecule causes an increase in the O—H bond strength and enhancement of the acid properties of the ROOH compounds. Compound **3** is well known[55] to be a weak acid, which readily forms peroxides CF_3OOR with various reagents. The O—O bond strength in the CF_3OOH molecule calculated using the ΔH_f° values obtained in this work is 215.0 kJ mol^{-1}, which is in agreement with the known stability of **3**.

Vibrational spectra. Taking peroxides **1** and **4** as examples, we showed that the computational methods employed in this study predict close values of the vibrational frequencies. Therefore, we present the vibrational spectra of peroxides **2** and **5** obtained from MP2 calculations only (Tables 3 and 4, respectively). In the calculated spectra the vibrations with frequencies higher than 1300 cm^{-1} correspond to the stretching and bending vibrations of the C—H bonds, except for the ν(OH) vibration in molecule **2**.

Two bands correspond to the stretching vibrations of the O—O bond. The ν(OO) vibration makes the predominant contribution to the vibrations with frequencies of 832 (**2**) and 827 cm^{-1} (**5**), which permits the assignment of the corresponding bands to the peroxide bond vibration. The intensities of these bands in the IR spectrum are low, which is in agreement with the experimental data.[9,56,57] The bands at 881 (**2**) and 890 cm^{-1} (**5**) correspond to the vibrations of the C—O bond with the contributions from the ν(OO) vibration of 28 and 10%, respectively.

The band at 1276 cm^{-1} corresponds to the vibrations of the O—O—H bond angle. This band in the IR spectrum is of rather high intensity; however, its practical use as a "fingerprint" and for analytical purposes is precluded by the intense bands of the bending vibrations of adjacent bonds, which appear in the same spectral region.

Table 3. Vibrational spectrum of *tert*-butyl hydroperoxide **2** obtained from MP2 calculations

Vibration	*I**	ν**/cm^{-1}	PED
1	0.09	137	99τ(CO)
2	0.03	216	86τ(CC)
3	0.86	250	98τ(CC)
4	0.76	260	99τ(CC)
5	0.26	268	66τ(OO), 15δ(CCC)
6	1.19	282	39δ(COO), 39δ(CCO)
7	0.10	330	35δ(CCO), 24δ(CCC)
8	0.03	346	59δ(CCC), 35δ(CCO)
9	0.01	389	68δ(CCC), 15δ(CCO)
10	0.19	443	52δ(CCO), 29δ(CCC)
11	0.12	504	38δ(COO), 20δ(CCO)
12	0.05	722	69ν(CC), 11ν(CO)
13	0.20	832	68ν(OO), 13ν(CC)
14	0.13	881	41ν(CC), 32δ(CCH)
15	0.00	899	63ν(CC), 33δ(CCH)
16	0.00	907	36δ(CCH), 30ν(CO)
17	0.00	929	90δ(CCH)
18	0.01	1010	82δ(CCH)
19	0.02	1016	82δ(CCH)
20	0.69	1202	47δ(CCH), 40ν(CC)
21	0.38	1238	51δ(CCH), 28ν(CC)
22	0.98	1242	41ν(CO), 26δ(CCH)
23	1.00	1276	92δ(OOH)
42	0.77	3601	99ν(OH)

* Intensity of the corresponding vibration/D^2 a.m.u.$^{-1}$ Å^{-2}.
** The remaining frequencies are as follows: 1352, 1355, 1376, 1434, 1449, 1451, 1458, 1461, 1483, 2939, 2942, 2951, 3029, 3033, 3037, 3043, 3046, and 3051 cm^{-1}.

The calculated frequencies of the stretching vibrations of the C—O bond are 881 cm^{-1} for *tert*-butyl hydroperoxide and 872 (asymmetrical) and 890 cm^{-1} (symmetrical) for di-*tert*-butyl peroxide. The contribution of ν(CO) to the other bands in the vibrational spectra of the peroxides **2** (722, 832, and 1202 cm^{-1}) and **5** (728, 1192, and 1205 cm^{-1}) varies from nearly 10 to 18%. It is remarkable that, similarly to molecule **4**, the asymmetrical vibration of the C—O bond in molecule **5** appears at a lower frequency.

The frequency of the torsional vibration associated with rotation about the peroxide bond in molecule **2** is 282 cm^{-1}. The frequency of the corresponding vibration in molecule **5** is apparently determined with a large absolute error (calculations give a τ(OO) frequency of 15 cm^{-1}). The reason is the substantially flattened dependence of the energy of this molecule on the C—O—O—C dihedral angle. The assignments of other bands of peroxides **2** and **5** are listed in Tables 3 and 4, respectively.

Table 4. Vibrational spectrum of di-*tert*-butyl peroxide **5** calculated by the MP2 method

Vibration	*I**	ν**/cm^{-1}	PED
1	0.01	15	57τ(OO), 40τ(CO)
2	0.03	58	59τ(CO), 45τ(OO)
3	0.03	105	46τ(CO), 41δ(COO)
4	0.01	167	57τ(CC), 20δ(COO)
5	0.00	183	97τ(CC)
6	0.01	199	57τ(CC), 25τ(CO)
7	0.00	228	42δ(CCO), 35δ(COO)
8	0.00	243	91τ(CC)
9	0.00	252	85τ(CC), 10δ(CCO)
10	0.00	254	86τ(CC)
11	0.01	262	93τ(CC)
12	0.00	270	56δ(CCO), 15τ(CC)
13	0.01	324	51τ(CO), 39δ(CCO)
14	0.05	334	55τ(CO), 35δ(CCO)
15	0.01	338	67τ(CO), 18δ(CCO)
16	0.00	386	66τ(CO), 16δ(CCO)
17	0.03	404	81δ(CCO)
18	0.19	441	54δ(CCO), 30τ(CO)
19	0.05	443	45δ(CCO), 38τ(CO)
20	0.02	487	37δ(CCO), 22δ(COO)
21	0.14	508	39δ(CCO), 22δ(COO)
22	0.23	728	79ν(CC), 19ν(CO)
23	0.00	747	79ν(CC)
24	0.00	827	63ν(OO), 11δ(COO)
25	0.88	872	64ν(CO), 23δ(CCH)
26	0.01	890	46ν(CO), 20δ(CCH)
27	0.00	894	49δ(CCH), 40ν(CC)
28	0.00	894	52δ(CCH), 41ν(CC)
29	0.03	905	55δ(CCH), 37ν(CC)
30	0.00	907	52δ(CCH), 30ν(CC)
31	0.00	924	84δ(CCH), 16τ(CC)
32	0.00	924	84δ(CCH), 16τ(CC)
33	0.02	1007	71δ(CCH), 12τ(CC)
34	0.01	1008	70δ(CCH), 12τ(CC)
35	0.04	1009	71δ(CCH), 12τ(CC)
36	0.00	1021	69δ(CCH), 12τ(CC)
37	3.70	1192	43δ(CCH), 20τ(CC)
38	0.03	1205	44δ(CCH), 20τ(CC)
39	0.05	1232	35δ(CCH), 33ν(CC)
40	0.54	1233	34δ(CCH), 33ν(CC)
41	0.38	1241	33ν(CC), 32δ(CCH)
42	0.01	1261	32δ(CCH), 28ν(CC)

* See note* to Table 3.

** The remaining frequencies are as follows: 1349, 1350, 1351, 1352, 1372, 1373, 1431, 1431, 1443, 1446, 1446, 1449, 1454, 1455, 1458, 1458, 1477, 1479, 2920, 2920, 2924, 2924, 2929, 2930, 3008, 3008, 3014, 3015, 3018, 3020, 3033, 3033, 3037, 3037, 3044, and 3045 cm^{-1}.

The results obtained are by and large in good agreement with the literature data,[9,56,57] according to which characteristic of the peroxide molecules are the bands at 3600 (ν(OH)) and 840 cm^{-1} (ν(OO)) in the IR spectra and the lines at 3600, 880 (ν(CC)), 840, 720 (ν(CC)), 520—590, and 230—280 cm^{-1} in the Raman spectra. Discrepancies between the assignments were found only for the stretching vibration of the C—O bond, which corresponds[9,56,57] to the IR bands and Raman lines in the range 1209—1246 cm^{-1}.

Table 5 lists the results of MP2 calculations of the vibrational spectra of the fluorine-containing peroxides **3**

Table 5. Vibrational spectra of the fluorine-containing peroxides **3** and **6** obtained from MP2 calculations

I[a]	0.937(ν/cm^{-1})	PED	Reference data
		CF_3OOH (**3**)[b]	
0.22	131	90τ(CO)	142[c]
2.44	221	77τ(OO)	246[c]
0.54	265	51δ(COO), 36δ(FCO)	290[c]
0.09	406	63δ(FCO), 33τ(CO)	
0.04	419	45δ(FCO), 29τ(CO)	
0.08	549	31δ(FCO), 42τ(CO)	
0.16	577	53τ(CO), 23δ(FCO)	613 w
0.25	638	46δ(FCO), 21ν(CF)	675 m
0.02	827	52ν(CF), 21ν(CO)	
0.24	919	67ν(OO), 19ν(CF)	945 m
8.25	1196	48ν(CF), 25ν(CO)	1140 w
9.06	1223	52ν(CF), 26ν(CO)	1238 vs
7.96	1257	73ν(CF), 15τ(CO)	1268 s
1.90	1324	91δ(OOH)	1382 m
1.06	3595	100ν(OH)	3580 m
		CF_3OOCF_3 (**6**)[d]	
0.00	55	89τ(CO)	67
0.00	87	75τ(CO), 20δ(COO)	85
0.00	93	96τ(OO)	92
0.02	207	42δ(COO), 40δ(FCO)	215
0.00	218	58δ(COO), 31δ(FCO)	232
0.00	323	75δ(FCO), 14ν(OO)	344
0.00	404	73δ(FCO), 27τ(CO)	
0.00	414	61δ(FCO), 32τ(CO)	445
0.08	458	56τ(CO), 30δ(FCO)	490
0.02	527	71τ(CO), 12ν(CF)	559
0.16	570	59τ(CO), 22δ(FCO)	610
0.14	576	54τ(CO), 25δ(FCO)	627
0.36	586	74δ(FCO), 15ν(CO)	634
0.12	642	30τ(CO), 27δ(FCO)	673
0.20	662	52δ(FCO), 23ν(CF)	711
0.01	834	41ν(CF), 20ν(OO)	890
0.05	843	66ν(CF), 34ν(CO)	
0.04	933	58ν(OO), 23ν(CF)	975
17.36	1137	49ν(CO), 29ν(CF)	1125
5.91	1211	80ν(CF), 14τ(CO)	1166
1.66	1224	42ν(OO), 33ν(CF)	1240
10.54	1242	79ν(CF), 15τ(CO)	1252
14.14	1263	78ν(CF), 16τ(CO)	1265
2.86	1279	67ν(CF), 13τ(CO)	1303

[a] See note* to Table 1.

[b] The experimental data were taken from Ref. 55.

[c] See Ref. 58.

[d] The experimental data were taken from Refs. 59—61.

and **6**, which predict a strong intensity for the torsional vibration of the O—O bond at 221 cm^{-1} in the IR spectrum of **3**. Indeed, it was reported[58] that the intensity of the τ(OO) vibration is so high that this absorption covers the spectral region 200—300 cm^{-1}. The ν(OH) and δ(OOH) vibrations are well-localized and have rather high intensities in the IR spectrum; however, they were characterized[55] as vibrations of medium intensity against the background of the very intense absorption of the C—F bonds. Noteworthy is that the spectrum of molecule **3** exhibits no band which could be formally attributed to the ν(CO) vibration because of the strong mixing with the vibrations of the C—F bonds.

In addition to the intense C—F absorption bands in the region 1211—1279 cm^{-1} the IR spectrum of molecule **6** contains vibrations of the C—O bond at 1224 cm^{-1} (ν^{s}) and 1137 cm^{-1} (ν^{as}). The last-named vibration is the most intense in the IR spectrum and, similarly to other dialkyl peroxides (see above), has the lower frequency.

The stretching vibrations of the O—O bond in the molecules of fluorine-containing peroxides are of low intensity in the IR spectra analogously to the other molecules. In contrast to this, the corresponding bands in the Raman spectra are the strongest ones, which permits the ν(OO) values to be used for identification of peroxides.[62] A feature of the spectra of molecules **3** and **6** is shift of the frequency of the ν(OO) vibration to the region 919—933 cm^{-1} as compared to the spectra of molecules **2**, **5** (827—832 cm^{-1}) and **1**, **4** (772—815 cm^{-1}). This is due to the mixing of the vibrations of the O—O and C—F bonds (see Table 5).

Conformational flexibility under rotation about the O—O bond. According to calculations, all the compounds under study have stable structures characterized by the *gauche*-arrangement of substituents with respect to the peroxide bond (see Fig. 1). The potential curves of internal rotation about the peroxide bond (Fig. 2) exhibit two barriers, of which the higher, *cis*-barrier, corresponds to the planar configuration of the C—O—O—C/H fragment in which the substituents are arranged on one side with respect to the O—O bond. The heights of the *cis*- and *trans*-barriers are listed in Table 1.

As the φ angle changes from 0 to 180°, the C—O—O bond angles monotonically decrease. For instance, the C—O—O angle in molecule **2** changes in the range 113.3—107.4°, while the O—O—H angle changes from 104.3 to 97.6°. The most reasonable explanation for this effect is a decrease in the energy of steric repulsion between substituents at the peroxide fragment with an increase in the torsion angle φ.

The C—O and O—O bond lengths change in a more complex way (Fig. 3). In all the peroxides under study the C—O bond is lengthened in a regular manner at a nearly orthogonal arrangement of the planes passing through the C, O, O atoms and the O, O, C/H atoms. The *d*(C—O) value depends on the nearest bonding environment and the maximum C—O bond length corresponds to φ = 95±20°. The O—O bond length changes in antiparallel manner, namely, the minimum *d*(O—O) value corresponds to φ = 85±20°.

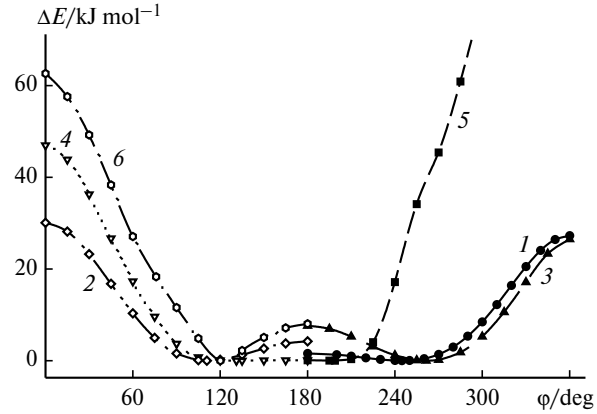

Fig. 2. Potential curves of internal rotation of alkyl groups about the O—O bond in molecules **1—6** (curves *1—6*, respectively) obtained from B3LYP/6-31G(d,p) calculations. From symmetry considerations the curves are presented for the 180° interval.

A minimum in the *d*(O—O) plot in Fig. 3 points to stabilization of the peroxide bond at virtually orthogonal arrangement of substituents at this bond. Since the low strength of the O—O bond is determined by repulsion between the lone electron pairs (LEP) of O atoms, shortening of the O—O bond indicates that the LEP are involved in the orbital interactions with transfer of the electron density to adjacent atoms. This reduces the populations of the nonbonding orbitals of the O atoms and, hence, weakens repulsion between the LEP, thus stabilizing the *gauche*-conformation of the molecule.

The orbital interactions in the peroxide molecules were analyzed in the framework of the natural bonding orbital (NBO) approach.[23] The energies of the most important interactions occurring in the stable conformations of the peroxide molecules under study, as well as the populations of the occupied and unoccupied orbitals are listed in Table 6. Changes in the φ angle affects the mutual orientation of the LEP of the O atoms and the adjacent polar bonds, the energy of hyperconjugation between the n_{π}-orbitals and the antibonding orbitals of the adjacent C—O (and O—H) bonds being changed parallel to the change in the C—O bond lengths and antiparrallel to the change in the *d*(O—O) value (see Fig. 3).

The determining role of the interaction between the n_{π}-orbitals and the orbitals of the adjacent polar bonds in stabilization of the *gauche*-conformation of the peroxide molecule is illustrated by the plot of the energy of the $n_{\pi} \rightarrow \sigma^{*}$(C—O) interaction *vs.* the torsion angle φ for the stable conformations of all the molecules under study (Fig. 4). As can be seen in Fig. 4, the stabilizing effects counteract some other interactions, which provide a broad

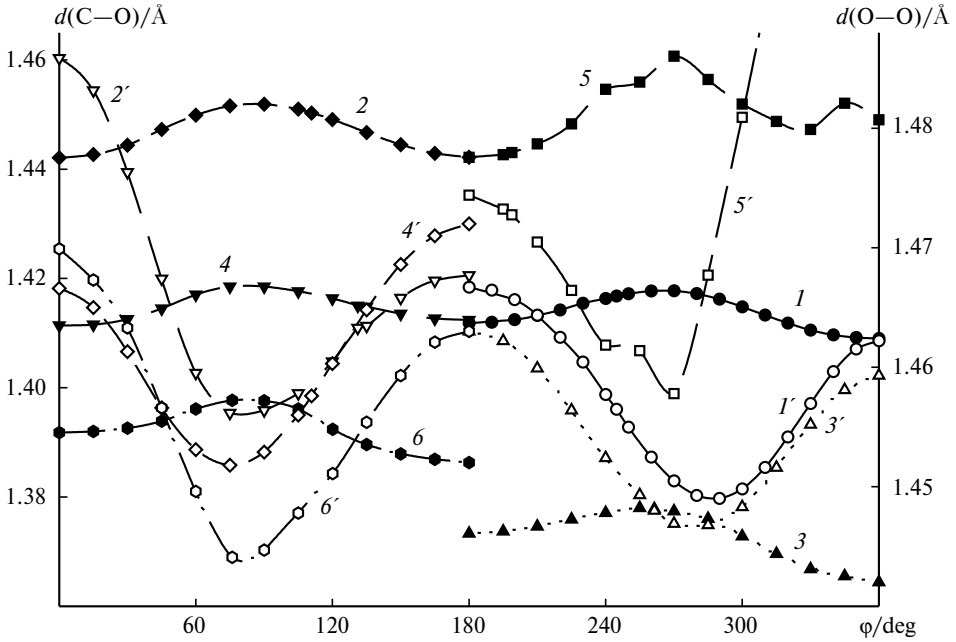

Fig. 3. Changes in the C—O bond lengths (*1*—*6*, black symbols) and O—O bond lengths (*1′*—*6′*, white symbols) under internal rotation of alkyl groups about the O—O bond in the molecules **1** (*1*, *1′*), **2** (*2*, *2′*), **3** (*3*, *3′*), **4** (*4*, *4′*), **5** (*5*, *5′*), and **6** (*6*, *6′*). Calculated by the B3LYP/6-31G(d,p) method. From symmetry considerations the curves are presented for the 180° interval.

range of the φ values. Let us consider qualitatively the main orbital interactions at different values of the C—O—O—R torsion angle assuming that the LEP is the n_σ, n_π pair.

The LEP orientation in the cisoid conformation of the molecule is the least favorable (Scheme 1).

Repulsion between the LEP is maximum, while the orientation of the n_π-orbitals makes their interaction with the adjacent bonds impossible. The peroxide molecule can be to some extent stabilized only due to the $n_\sigma \rightarrow \sigma^*$(O—R) interaction.

In addition, a feature of the *cis*-conformer is steric repulsion between the C and R atoms, which substantially increases for the bulky substituents. Therefore, the above-mentioned factors are responsible for instability of the *cis*-conformer. Repulsion between the LEP causes an in-

Table 6. Energies of the orbital interactions (in kJ mol^{-1}) and the populations of the interacting orbitals (in *e* units)

Parameter	MeOOH (**1**), X = H, R = H	Bu^{t}OOH (**2**), X = C, R = H	CF_3OOH (**3**), X = F, R = H	MeOOMe (**4**), X = H, R = C	Bu^{t}OOBu^t (**5**), X = C, R = C	CF_3OOCF_3 (**6**), X = F, R = C
Interaction energy						
$n_\pi(O_\alpha) \rightarrow \sigma^*(O_\beta—R)$	3.5	3.8	4.4	2.1	~0	4.5
$n_\pi(O_\beta) \rightarrow \sigma^*(O_\alpha—C)$	5.4	5.5	9.0	2.1	~0	4.5
$n_\pi(O_\alpha) \rightarrow \sigma^*(C—X_a)$	22.4	20.8	56.0	24.0	24.5	51.2
$n_\pi(O_\alpha) \rightarrow \sigma^*(C—X_s)$	27.5	25.2	61.0	26.6	23.3	54.3
$\sigma(O_\alpha—O_\beta) \rightarrow \sigma^*(C—X_t)$	8.0	7.0	18.7	7.9	7.3	15.6
$\sigma(C—X_t) \rightarrow \sigma^*(O_\alpha—O_\beta)$	22.0	17.2	8.8	21.0	16.8	9.1
Population						
$\sigma(O_\alpha—O_\beta)$	1.9919	1.9921	1.9837	1.9864	1.9863	1.9749
$\sigma(C—X_t)$	1.9784	1.9682	1.9910	1.9783	1.9681	1.9906
$n_\pi(O_\alpha)$	1.9590	1.9606	1.9143	1.9564	1.9588	1.9206
$n_\pi(O_\beta)$	1.9907	1.9869	1.9869	1.9564	1.9588	1.9206
$\sigma^*(O_\alpha—O_\beta)$	0.0240	0.0246	0.0185	0.0442	0.0453	0.0379
$\sigma^*(O_\beta—R)$	0.0040	0.0041	0.0052	0.0052	0.0488	0.1142
$\sigma^*(O_\alpha—C)$	0.0062	0.0540	0.1069	0.0052	0.0488	0.1142
$\sigma^*(C—X_a)$	0.0199	0.0309	0.1269	0.0208	0.0322	0.1248
$\sigma^*(C—X_s)$	0.0216	0.0320	0.1340	0.0212	0.0325	0.1262
$\sigma^*(C—X_t)$	0.0088	0.0222	0.1110	0.0082	0.0216	0.1099

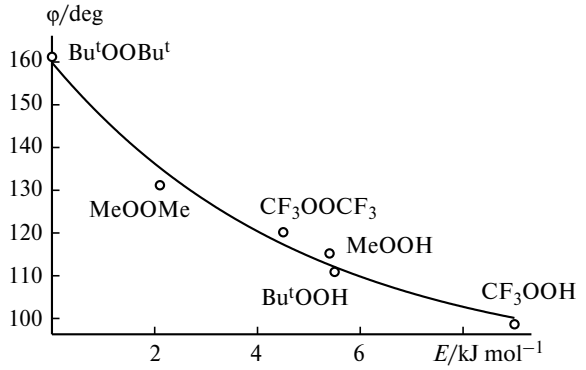

Fig. 4. Correlation between the torsion angle φ in the stable conformations of peroxide molecules and the energy of the $n_\pi(O_\beta) \rightarrow \sigma^*(O_\alpha—C)$ interaction.

Scheme 1

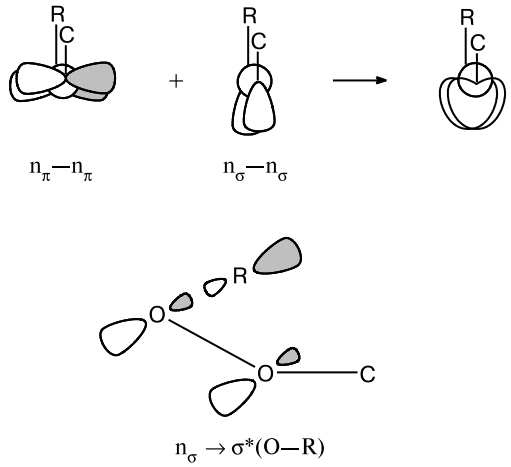

crease in the O—O bond length, which reaches its maximum value in the *cis*-conformer (see Fig. 3).

The other top of the potential barrier corresponds to the *trans*-conformation of the peroxide molecule. Similarly to the preceding case, the reason is that the LEP of the O atoms cannot be involved in the interactions with the orbitals of adjacent bonds (Scheme 2).

Scheme 2

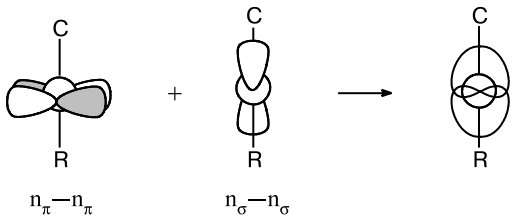

At the same time the *trans*-orientation of the peroxide fragment is optimum from the standpoint of minimization of the steric effects of substituents. The mutual arrangement of the LEP is also favorable. Taken altogether, these reasons provide an explanation for the low energy of the *trans*-barrier.

In the case of orthogonal arrangement of the C and R substituents the energy of repulsion between the LEP takes an intermediate value because of the $n_\pi—n_\sigma$ pair interaction. However, the *gauche*-conformation is favorable for involvement of both n_π-orbitals in the overlap with the σ*-orbitals of adjacent bonds (Scheme 3).

Scheme 3

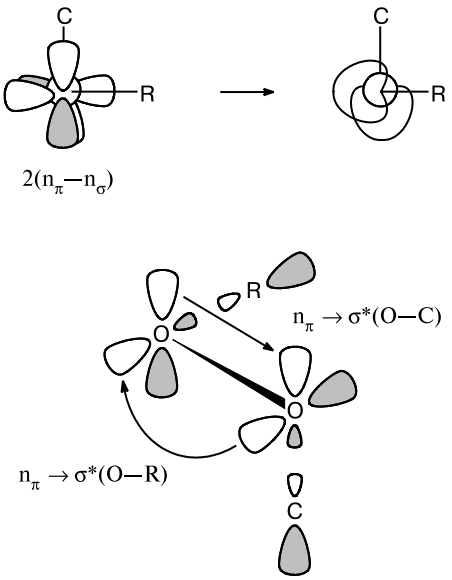

The plots of *d*(O—O) *vs.* the C—O—O—X torsion angle (see Fig. 3) exhibit clearly seen minima at φ ~90°. Due to hyperconjugation and electron density transfer from the LEP to other orbitals the O—O bond order increases and repulsion between the LEP weakens, thus causing the O—O bond to shorten. At the same time the effective $n_\pi \rightarrow \sigma^*(C—O)$ interaction leads to an increase in the population of the antibonding orbital and destabilizes the C—O bond *via* its elongation. Indeed, Fig. 3 demonstrates that at φ ~90° the *d*(C—O) values increase by about 0.01—0.02 Å.

However, orthogonal arrangement of the C and R substituents is not optimum from the standpoint of the interaction between the LEP of adjacent O atoms. If we assume that steric repulsion between the Bu^t group and the H atom in molecule **2** is minimum, an increase in the φ value to 110.9° is due to the repulsion between the LEP. Mutual repulsion between the bulky substituents in molecule **5** leads to even greater increase in the φ angle.

Thus, the conformational potential of peroxide compounds with different structure is determined by three main factors:

1) hyperconjugation between the LEP of the atoms of the peroxide bridge and the antibonding σ*-orbitals of the adjacent C—O (or O—H) bonds,

2) Coulomb repulsion between the LEP,

3) steric interaction of substituents at the peroxide bond.

The first effect is responsible for the stability of the *gauche*-structure of the peroxide fragment. It is maximum at φ ~80° irrespective of the nature of the peroxide compound. The second and third effects cause destabilization of the peroxide molecule, thus leading to an increase in the φ angle.

The key role of the LEP of O atoms in the formation of the conformational potential of peroxide molecules points to a great importance of taking into account nonvalent interactions. The orbital effects, as well as the interaction between the O—O group and the electron shells of the α-, β-, and even γ-C atoms (as detected in the NMR spectra) show[3] that homolysis of the O—O bond in the course of decomposition of the peroxide compounds is a process, which also involves the electron orbitals of adjacent atoms and functional groups, rather than an elementary act. It is the orbital interactions that are responsible for the variety of thermal decomposition mechanisms and for a broad range of changes in the O—O bond strength.

The d-effect. A peculiar feature of the structure of alkyl peroxide molecules is distortion of the tetrahedral configuration of the X_3CO fragment (the so-called distortion effect, or d-effect).[28] The d-effect is typical of all alkyl peroxides and alkylaryl peroxides[8] and also manifests itself in alcohols and esters, which points to the determining role of the O atom nearest to the X_3C group (O_α atom).

The most characteristic manifestation of the d-effect is a substantial decrease in the X—C—O bond angle for the X_t atom in the transoid position with respect to the O_β atom of the peroxide group (see Fig. 1). For instance, if the $\theta(X_a)$ and $\theta(X_s)$ angles in molecule **1** are close to the tetrahedral angle (110.01 and 111.38°, respectively), the $\theta(X_t)$ angle is much smaller (104.32°). Even more pronounced is the d-effect in molecule **4**; according to MP2 calculations, $\theta(X_t)$ = 101.48°, $\theta(X_a)$ = 109.89°, and $\theta(X_s)$ = 110.60°. The X—C—O bond angles in these and other peroxides are listed in Table 7.

To elucidate the nature of the d-effect, we used the results of the NBO analysis of the peroxide molecules. It was found that free rotation about the O—O bond does not influence the d-effect. The H—C—O bond angles in molecule **1** change only slightly (by 0.5—0.6°). The largest contribution to the d-effect comes from the occupied orbitals σ(C—H_t) (1.9784), σ(O—O) (1.9919), and $n_\pi(O_\alpha)$ (1.9590), which interact with the σ*(C—H_t) (0.0088), σ*(C—H_a) (0.0199), σ*(C—H_s) (0.0216), and σ*(O—O) (0.0240) antibonding orbitals (the populations of the corresponding orbitals are given in parentheses). Analogous trends were also found for the remaining peroxides (see Table 6).

From this it follows that the d-effect is due to the orbital interactions involving the transoid X atom (the

Table 7. Influence of substituents on the magnitude of the d-effect (change in the bond angle (deg)) in the compounds of general formula X_3CZY according to the results of MP2/6-31G(d,p) calculations

Compound*	X_t	X_a	X_s	Z	Y	Z—C—H_t	Z—C—H_a	Z—C—H_s	C—Z—Y
CF_3OOCF_3	F	F	F	O	CF_3O	104.0	111.7	112.4	105.0
Bu^tOOBu^t	C	C	C	O	Bu^tO	101.5	109.9	110.6	106.1
CF_3OOH	F	F	F	O	OH	105.1	112.8	111.8	105.6
Bu^tOOH	C	C	C	O	OH	101.5	110.0	110.3	107.7
Me_2CHOOH [52]	C	H	C	O	OH	103.7	108.0	111.5	106.1
CCl_3OOH [63]	Cl	Cl	Cl	O	OH	102.3	111.0	112.0	107.6
$CHCl_2OOH$ [63]	H	Cl	Cl	O	OH	103.4	113.3	112.1	108.3
CH_2ClOOH [63]	H	H	Cl	O	OH	104.9	111.4	112.7	106.2
$MeONO_2$	H	H	H	O	NO_2	102.9	110.1	110.1	112.3
MeOF	H	H	H	O	F	103.2	111.0	111.0	103.2
MeOCl	H	H	H	O	Cl	103.6	111.5	111.5	109.3
MeOOC(O)Me	H	H	H	O	MeC(O)O	103.5	110.9	111.1	106.1
MeONO	H	H	H	O	NO	104.0	110.7	110.7	114.4
MeOOMe	H	H	H	O	MeO	104.4	111.0	111.4	104.3
MeOOH	H	H	H	O	OH	104.3	111.0	111.4	104.5
MeOH	H	H	H	O	H	106.5	112.4	112.4	107.3
MeOMe	H	H	H	O	Me	107.0	111.5	111.5	110.9
MeSSMe	H	H	H	S	MeS	106.7	110.8	110.5	102.0
MeSH	H	H	H	S	H	106.7	111.6	111.6	96.5
MeSMe	H	H	H	S	Me	107.7	111.3	111.3	98.5

* The data were obtained in this study unless otherwise stated.

$\sigma(C—X_t) \rightarrow \sigma^*(O—O)$ and $\sigma(O—O) \rightarrow \sigma^*(C—X_t)$ interactions) and the *gauche*-atoms (the $n_\pi(O_\alpha) \rightarrow \sigma^*(C—X_a)$ and $n_\pi(O_\alpha) \rightarrow \sigma^*(C—X_s$ interactions). The energies of these interactions are listed in Table 6, from which it follows that the d-effect originates from the interactions of the O_α atom.

The role of the O_β atom can be illustrated by the data listed in Table 7. Here we compare the bond angles in the compounds of general formula H_3COY, where Y is an atom or radical with different electron-acceptor ability. For the sake of comparison Table 7 also presents the geometric parameters of the sulfur-containing compounds. The data listed in Table 7 were obtained by the authors of this work using the results of MP2/6-31G(d,p) calculations and from the NIST quantum-chemical database.[52]

As the electron-acceptor properties of the Y substituent become stronger, the $O—C—H_t$ angle regularly decreases (Fig. 5). This effect can be explained with ease taking into account a decrease in the energy of the $\sigma^*(O—Y)$ orbital with an increase in the electronegativity of the Y substituent. As a result, the energy difference between the $\sigma(C—H_t)$ and $\sigma^*(O—Y)$ orbitals decreases, which makes the interaction of these orbitals more efficient. The energy of the other interaction, $n_\pi \rightarrow \sigma^*(C—H_g)$, does not change in this series of compounds. Indeed, the $O—C—H_g$ angle in all the H_3COY molecules has a nearly constant value (111.4±1°), whereas the $O—C—H_t$ angle changes from 102.9° (Y = NO_2) to 107.0° (Y = Me).

Noteworthy is that the $\sigma(C—H_t) \rightarrow \sigma^*(O—Y)$ and $\sigma(O—Y) \rightarrow \sigma^*(C—H_t)$ interactions can be efficient only if the O—Y and $C—H_t$ bonds are aligned. Indeed, this holds for the molecules characterized by the weakest steric interaction between H_g and Y (Y = H, F, OH, OMe) and manifests itself as the nearly equal values of the $O—C—H_t$ and C—O—Y bond angles (see Table 7), which differ by less than 1°.

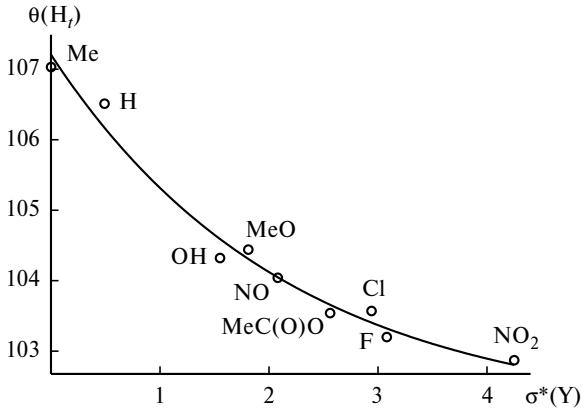

Fig. 5. Plot of the bond angle, $\theta(H_t)$, *vs.* the Taft inductive constants, σ*, of the substituent Y in the compounds of general formula H_3COY.

Replacement of the O_α atom by S atom leads to appreciable weakening of the d-effect (see Table 7), which is due to the lower donor ability of the LEP of S atom.

The influence of the X atom in the *gauche*-position on the strength of the d-effect is ambiguous. On the one hand, an increase in the electronegativity of X causes an increase in the energy of the $n_\pi \rightarrow \sigma^*(C—X_g)$ interaction (see Table 6), which manifests itself as an increase in the $O—C—X_g$ angle (see Table 7). On the other hand, bulky substituents in the *gauche*-position with respect to the O_β atom produce steric strain in the molecule, which is mainly manifested as an increase in the C—O—O angle.

If substituents at the C_α atom are different, the *gauche*-position relative to the O_β atom is occupied by the substituents with greater electronegativity while the transoid position is occupied by the electron-donor atom or radical (see Table 7, Me_2CHOOH, $ClCH_2OOH$, and Cl_2CHOOH). This trend becomes understandable in the light of the above-mentioned results and is associated with the overall effect of the $n_\pi \rightarrow \sigma^*(C—X_g)$ and $\sigma(C—X_t) \rightarrow \sigma^*(O—O)$ interactions under rotation of the X_3C fragment about the C—O bond.

The results obtained in this work are in agreement with the data collected in the experimental studies of the structure of peroxides. X-Ray diffraction studies of the structure of diphenylmethyl hydroperoxide, Ph_2CHOOH,[64] and dicumyl peroxide, $PhMe_2COOCMe_2Ph$,[65] pointed out that in both compounds the Ph rings are in the *gauche*-position with respect to the O_β atom despite obvious unfavorableness of this spatial orientation.

According to our calculations, the alkoxy radicals $X_3CO^\bullet$ (products of peroxide homolysis at the O—O bond) must correspond to the C_s rather than C_{3v} point symmetry group owing to the $n_\pi \rightarrow \sigma^*(C—X)$ interaction. Analysis of the published data[43,45,47,52] taking $MeO^\bullet$, $Bu^tO^\bullet$, $CF_3O^\bullet$, and other alkoxy radicals as examples shows that this does occur.

Thus, the structure of the most stable conformers of the peroxide and alkyl hydroperoxide molecules, ROOR´, is determined by superposition of several effects. These are repulsion between the LEP, stabilization of substituents at the peroxide group in the *gauche*-conformation (the anomeric effect), steric repulsion between the R and R´ substituents, and the d-effect. The nature of the R and R´ substituents influences the relative contribution of each factor. As the electronegativity of the X atom increases, the energy of the $\sigma^*(C—X)$ orbital decreases, the overlap with the n_π-orbital becomes more efficient and, hence, the population of the n_π-orbital decreases. The energy of repulsion between the LEP of O atoms also decreases. This effect correlates with the change in the O—O bond lengths (see Fig. 3). Namely, as the electron-acceptor properties of the X substituent in hydroperoxides X_3COOH become stronger (Me < H < F), the d(O—O) values cor-

respondingly decrease: 1.458 > 1.456 > 1.448 Å. An analogous trend can also be followed for the C—O bond (see Fig. 3). Weakening of repulsion between the LEP, which destabilizes the peroxide molecule, also manifests itself as a decrease in the torsion angle φ.

The authors express their gratitude to A. F. Khalizov and A. B. Ryzhkov for valuable help.

References

1. *Organic Peroxides*, Ed. D. Swern, Wiley, New York, 1970, **1**, 1971, 654 pp.; **2**, 963 pp.; 1972, **3**, 384 pp.
2. V. L. Antonovsky, *Organicheskie perekisnye initsiatory* [*Organic Peroxide Initiators*], Khimiya, Moscow, 1972, 448 pp. (in Russian).
3. V. L. Antonovsky and M. M. Buzlanova, *Analiticheskaya khimiya organicheskikh peroksidnykh soedinenii* [*Analytical Chemistry of Organic Peroxides*], Khimiya, Moscow, 1978, 308 pp. (in Russian).
4. V. L. Antonovsky, *Khimicheskie istochniki svobodnykh radikalov* [*Chemical Sources of Free Radicals*], Znanie, Moscow, 1980, 64 pp. (in Russian).
5. *The Chemistry of Peroxides*, Ed. S. Patai, Wiley, New York, 1983.
6. V. L. Antonovsky, *Khimiya peroksinitratov — komponentov fotokhimicheskogo smoga* [*Chemistry of Peroxy Nitrates, the Components of Photochemical Smog*], Nauka, Moscow, 1989, 109 pp. (in Russian).
7. *Organic Peroxides*, Ed. W. Ando, Wiley, New York, 1992, 645 pp.
8. V. L. Antonovsky, in *Vestnik Nizhegorodskogo gos. un-ta im. N. I. Lobachevskogo* [*Bull. N. I. Lobachevky Nizhnii Novgorod State Univ.*], Ed. V. A. Dodonov, Izd-vo NNGU, Nizhnii Novgorod, 1996, 3 (in Russian).
9. G. A. Pitsevich, Diss. kand. fiz.-mat. nauk [Ph.D. Thesis (Phys./Math.)], Belarus State University, Minsk, 1985, 183 (in Russian).
10. Yu. Ya. Van-Chin-Syan and N. S. Kachurina, in *Vestnik Nizhegorodskogo gos. un-ta im. N. I. Lobachevskogo* [*Bull. N. I. Lobachevky Nizhnii Novgorod State Univ.*], Ed. V. A. Dodonov, Izd-vo NNGU, Nizhnii Novgorod, 1996, 29 (in Russian).
11. V. L. Antonovsky and K. V. Bozhenko, *Dokl. Akad. Nauk*, 1995, **343**, 337 [*Dokl. Chem.*, 1995 (Engl. Transl.)].
12. V. L. Antonovsky and K. V. Bozhenko, *Dokl. Akad. Nauk*, 1995, **345**, 196 [*Dokl. Chem.*, 1995 (Engl. Transl.)].
13. V. L. Antonovsky and K. V. Bozhenko, *Izv. Akad. Nauk, Ser. Khim.*, 1997, 684 [*Russ. Chem. Bull.*, 1997, **46**, 653 (Engl. Transl.)].
14. V. L. Antonovsky, K. V. Bozhenko, and D. Kh. Kitaeva, *Izv. Akad. Nauk, Ser. Khim.*, 1998, 600 [*Russ. Chem. Bull.*, 1998, **47**, 578 (Engl. Transl.)].
15. S. L. Khursan, D. A. Mikhailov, A. A. Gusmanov, and I. M. Borisov, *Zh. Fiz. Khim.*, 2001, **75**, 815 [*Russ. J. Phys. Chem.*, 2001, **75** (Engl. Transl.)].
16. S. L. Khursan and V. V. Shereshovets, *Kinet. Katal.*, 1999, **40**, 167 [*Kinet. Catal.*, 1999, **40** (Engl. Transl.)].
17. V. V. Shereshovets, S. L. Khursan, V. D. Komissarov, and G. A. Tolstikov, *Usp. Khim.*, 2001, **70**, 123 [*Russ. Chem. Rev.*, 2001, **70** (Engl. Transl.)].
18. S. L. Khursan and V. L. Antonovsky, *Dokl. Akad. Nauk*, 2002, **382**, 657 [*Dokl. Phys. Chem.*, 2002 (Engl. Transl.)].
19. M. W. Schmidt, K. K. Baldridge, J. A. Boatz, S. T. Elbert, M. S. Gordon, J. H. Jensen, S. Koseki, N. Matsunaga, K. A. Nguyen, S. J. Su, T. L. Windus, M. Dupuis, and J. A. Montgomery, *J. Comput. Chem.*, 1993, **14**, 1347.
20. M. J. Frisch, G. W. Trucks, H. B. Schlegel, G. E. Scuseria, M. A. Robb, J. R. Cheeseman, V. G. Zakrzewski, J. A. Montgomery, R. E. Stratmann, J. C. Burant, S. Dapprich, J. Millam, M. A. D. Daniels, K. N. Kudin, M. C. Strain, O. Farkas, J. Tomasi, V. Barone, M. Cossi, R. Cammi, B. Mennucci, C. Pomelli, C. Adamo, S. Clifford, J. Ochterski, G. A. Petersson, P. Y. Ayala, Q. Cui, K. Morokuma, D. K. Malick, A. D. Rabuck, K. Raghavachari, J. B. Foresman, J. Cioslowski, J. V. Ortiz, B. B. Stefanov, G. Liu, A. Liashenko, P. Piskorz, I. Komaromi, R. Gomperts, R. L. Martin, D. J. Fox, T. Keith, M. A. Al-Laham, C. Y. Peng, A. Nanayakkara, C. Gonzalez, M. Challacombe, P. M. W. Gill, B. G. Johnson, W. Chen, M. W. Wong, J. L. Andres, M. Head-Gordon, E. S. Replogle, and J. A. Pople, *GAUSSIAN-98 (Revision A.3)*, Gaussian, Inc., Pittsburgh (PA), 1998.
21. A. D. Becke, *J. Chem. Phys.*, 1993, **98**, 5648.
22. A. P. Scott and L. Radom, *J. Phys. Chem.*, 1996, **100**, 16502.
23. A. E. Reed, L. A. Curtiss, and F. Weinhold, *Chem. Rev.*, 1988, **88**, 899.
24. W. J. Hehre, L. Radom, P. v. R. Schleyer, and J. A. Pople, *Ab Initio Molecular Orbital Theory*, Wiley, New York—Chichester—Brisbane—Toronto—Singapore, 1986.
25. J. Koput, *J. Mol. Spectrosc.*, 1986, **115**, 438.
26. Yu. L. Slovokhotov, T. V. Timofeeva, M. Yu. Antipin, and Yu. T. Struchkov, *J. Mol. Struct.*, 1984, **112**, 127.
27. D. Christen, H.-G. Mack, and H. Oberhammer, *Tetrahedron*, 1988, **44**, 7363.
28. A. Yu. Kosnikov, V. L. Antonovsky, S. V. Lindeman, M. Yu. Antipin, Yu. T. Struchkov, N. A. Turovskii, and I. P. Zyat´kov, *Teor. Eksp. Khim.*, 1989, **25**, 82 [*Theor. Exp. Chem.*, 1989, **25** (Engl. Trans.)].
29. C. J. Marsden, D. D. DesMarteau, and L. S. Bartell, *Inorg. Chem.*, 1977, **16**, 2359.
30. C. J. Marsden, L. S. Bartell, and F. P. Diodati, *J. Mol. Struct.*, 1977, **39**, 253.
31. P. S. Nangia and S. W. Benson, *J. Phys. Chem.*, 1979, **83**, 1138.
32. G. Baker, J. H. Littlefair, R. Shaw, and J. C. J. Thynne, *J. Chem. Soc.*, 1965, 6970.
33. N. A. Kozlov and I. B. Rabinovich, *Tr. khim. khim. tekhnol.* [*Proc. Chem. Chem. Engng.*], 1964, **10**, 189 (in Russian).
34. Yu. Ya. Van-Chin-Syan, Yu. P. Pavlovskii, N. S. Kachurina, M. A. Dikii, Yu. V. Panchenko, and G. A. Petrovskaya, *Zh. Fiz. Khim.*, 1990, **64**, 553 [*J. Phys. Chem. USSR*, 1990, **64** (Engl. Transl.)].
35. T. J. Wallington, M. D. Hurley, W. F. Schneider, J. Sehested, and O. J. Nielsen, *Chem. Phys. Lett.*, 1994, **218**, 34.
36. K. O. Christe, *Spectrochim. Acta*, 1971, **27A**, 463.
37. M. E. Butwill Bell and J. Laane, *Spectrochim. Acta*, 1972, **28A**, 2239.

38. J. Koput, *Chem. Phys. Lett.*, 1995, **236**, 516.
39. S. W. Benson, *Oxid. Commun.*, 1982, **2**, 169.
40. V. L. Antonovsky, *Kinet. Katal.*, 1995, **36**, 370 [*Kinet. Catal.*, 1995, **36** (Engl. Transl.)].
41. W. F. Schneider and T. J. Wallington, *J. Phys. Chem.*, 1993, **97**, 12783.
42. R. Benassi, U. Folli, S. Sbardellati, and F. Taddei, *J. Comput. Chem.*, 1993, **14**, 379.
43. M. R. Zachariah, P. R. Westmoreland, D. R. Burgess, W. Tsang, and C. F. Melius, *J. Phys. Chem.*, 1996, **100**, 8737.
44. W. Reints, D. A. Pratt, H.-G. Korth, and P. Mulder, *J. Phys. Chem., A*, 2000, **104**, 10713.
45. W. G. Mallard and P. J. Linstrom, *NIST Chemistry WebBook, NIST Standard Reference Database Number 69*, National Institute of Standards and Technology, Gaithersburg (MD), February 2000.
46. J. B. Levy and R. C. Kennedy, *J. Am. Chem. Soc.*, 1972, **94**, 3302.
47. W. F. Schneider, B. I. Nance, and T. J. Wallington, *J. Am. Chem. Soc.*, 1995, **117**, 478.
48. D. A. Dixon and D. Feller, *J. Phys. Chem.*, 1998, **102**, 8209.
49. R. L. Asher, E. H. Appelman, and B. Ruscic, *J. Chem. Phys.*, 1996, **105**, 9781.
50. L. A. Curtiss, K. Raghavachari, G. W. Trucks, and J. A. Pople, *J. Chem. Phys.*, 1991, **94**, 7221.
51. L. A. Curtiss, K. Raghavachari, and J. A. Pople, *J. Chem. Phys.*, 1993, **98**, 1293.
52. *Computational Chemistry Comparison and Benchmark Database. Release 6a, NIST Standard Reference Database Number 101*, National Institute of Standards and Technology, Gaithersburg (MD), May 2002.
53. M. Jonsson, *J. Phys. Chem.*, 1996, **100**, 6814.
54. S. L. Khursan and V. V. Shereshovets, *Izv. Akad. Nauk, Ser. Khim.*, 1996, 327 [*Russ. Chem. Bull.*, 1996, **45**, 312 (Engl. Transl.)].
55. P. A. Bernstein, F. A. Hohorst, and D. D. DesMarteau, *J. Am. Chem. Soc.*, 1971, **93**, 3882.
56. I. P. Zyat´kov, Yu. A. Ol´dekop, A. P. Yuvchenko, N. M. Ksenofontova, G. A. Pitsevich, D. I. Sagaidak, V. I. Gogolinskii, and V. L. Antonovsky, *Zh. Prikl. Spektrosk.*, 1988, **48**, 585 [*J. Appl. Spectr. USSR*, 1988, **48** (Engl. Transl.)].
57. I. P. Zyat´kov, G. A. Pitsevich, A. P. Yuvchenko, Yu. A. Ol´dekop, V. I. Gogolinskii, V. L. Antonovsky, and D. I. Sagaidak, *Zh. Prikl. Spektrosk.*, 1989, **49**, 271 [*J. Appl. Spectr. USSR*, 1989, **49** (Engl. Transl.)].
58. R. M. Hammaker, W. G. Fateley, A. S. Manocha, D. D. DesMarteau, B. J. Streusand, and J. R. Durig, *J. Raman Spectrosc.*, 1980, **9**, 181.
59. J. R. Durig and D. W. Wertz, *J. Mol. Spectrosc.*, 1968, **25**, 467.
60. J. R. Durig, W. E. Bucy, and W. J. Natter, *J. Raman Spectrosc.*, 1977, **6**, 257.
61. C. J. Marsden, *J. Mol. Struct.*, 1981, **73**, 223.
62. A. J. Melveger, L. R. Anderson, C. T. Ratcliffe, and W. B. Fox, *Appl. Spectrosc.*, 1972, **26**, 381.
63. H. Sun, C.-J. Chen, and J. W. Bozzelli, *J. Phys. Chem., A*, 2000, **104**, 8270.
64. Yu. A. Kosnikov, V. L. Antonovsky, and S. V. Lindeman, *Kristallografiya*, 1989, **31**, 360 [*Crystallogr. Reports*, 1989, **31** (Engl. Transl.)].
65. Yu. A. Kosnikov, V. L. Antonovsky, N. A. Turovskii, S. V. Lindeman, T. V. Timofeeva, Yu. T. Struchkov, and I. P. Zyat´kov, *Izv. Akad. Nauk SSSR, Ser. Khim.*, 1988, 791 [*Bull. Acad. Sci. USSR, Div. Chem. Sci.*, 1988, **37**, 674 (Engl. Transl.)].

Received May 31, 2002;
in revised form December 23, 2002